Total-energy full-potential linearized augmented-plane-wave method for bulk solids: Electronic and structural properties of tungsten

H. J. F. Jansen and A. J. Freeman

Department of Physics and Astronomy, Northwestern University, Evanston, Illinois 60201

(Received 23 February 1984)

The development of the all-electron full-potential linearized augmented-plane-wave (FLAPW) method for bulk solids is reported. As in the thin-film FLAPW approach, the bulk FLAPW method solves the Kohn-Sham equations for a general charge density and potential. The formalism of Weinert, Wimmer, and Freeman for determining highly accurate total energies of solids within density-functional theory is implemented with all the necessary terms obtained from the FLAPW energy-band calculation. The resulting total-energy FLAPW approach is used to obtain highly accurate total-energy curves for bcc and fcc tungsten from which a number of structural properties (lattice parameters, bulk moduli, etc.) are derived. Calculated total energies have a relative precision of 0.1 mRy; a difference of 34 mRy is found between the (stable) bcc and fcc phases. The use of a simple quadratic form near the equilibrium value of the atomic volume is shown to lead to relatively large errors for the bulk modulus. Finally it is shown that in this all-electron method, all numerical approximations are controlled in that their effects can be minimized. One can therefore conclude that the FLAPW method is very well suited for testing the quality of various implementations of density-functional theory.

I. INTRODUCTION

The advent and application of highly sophisticated experimental methods for determining the multitudinous, and often exotic, properties of solids has brought a growing demand for detailed accurate theoretical information with which to critically analyze and interpret this rapidly growing body of information. As a result, considerable attention has been paid in recent years to quantum-mechanical theories which describe the dynamics of many-interacting electrons in an external potential, e.g., due to the atomic nuclei. An important breakthrough was the development of density-functional theory,[1] which states that under certain conditions all ground-state properties of an interacting electron gas are completely determined by the charge density of the electrons. In principle, density-functional theory permits the accurate evaluation of the electronic part of the total energy and, consequently, after including the Coulomb interaction between the nuclei it enables the evaluation of all structural properties.

At present, the most precise way to evaluate the electronic structure is to solve the Kohn-Sham equations[1] in the local-density approximation. However, in the period of time just after the development of density-functional theory the numerical methods for solving the Kohn-Sham equations were so crude that resulting errors completely obscured the effects of the physical approximations. Only recently has it become possible, due to enormously increased computer power and sophisticated combined theoretical and computational approaches, to solve these equations in a much more exact fashion.

An important advance in all-electron approaches was the recent development of the full-potential linearized augmented plane wave (FLAPW) method[2] for thin films. In this approach, a new technique for solving Poisson's equation[3] for a general charge density and potential is implemented; thus all contributions to the potential are completely taken into account in the Hamiltonian matrix elements. Results obtained for thin metal films and for nearly free molecules demonstrate the high degree of accuracy possible with this method.[2,4]

The development of accurate methods to solve the local-density equations has brought about increasing interest in using these methods to determine the total energy and related properties (such as equilibrium phases, lattice constants, and force constants) since the total energy is a fundamental quantity in density-functional theory. For all-electron methods there has been the major problem in evaluating the total-energy expression which arises from numerical problems introduced by the necessity of canceling the very large (positive) kinetic and large (negative) potential energy contributions. As is well known, this problem becomes very severe for heavy atoms since the core electrons are responsible for the largest part of the total energy. A successful solution of this difficulty has recently been presented in the form of a new formalism for determining highly accurate total energies of solids within density-functional theory. In this approach,[4] all necessary terms are easily obtained from the energy-band calculation. A major feature of this all-electron method is the explicit algebraic cancellation of the numerical Coulomb singularities in the kinetic and potential energy terms which leads to good numerical stability. As implemented in the FLAPW film approach,[4] the method allows one to treat the total energy of an all-electron system to high accuracy without resorting to frozen-core, pseudopotential, or other approximations.

The success of the FLAPW total-energy approach for thin films makes it very likely that a similar scheme for bulk materials would also provide us with reliable

structural information. In this paper we show that this is indeed the case.[5] Section II explains some basis details of our FLAPW method for bulk solids. In Sec. III we apply our method to fcc and bcc tungsten and show that we are able to make meaningful comparisons with experiment. Section IV draws our conclusions. In the Appendix we elaborate on a number of numerical convergence tests which were taken in order to establish the precision of our method.

II. METHOD

By far, a large majority of the accurate electronic structure calculations for solids is now carried out on the basis of density-functional theory.[1] In this approach, one assumes that it is possible to replace the N-particle equation describing the behavior of all electrons by a set of single-particle equations for a noninteracting electron gas in an external potential. These so-called Kohn-Sham equations[1] are

$$[K + v_{\text{eff}}(n,\vec{r})]\phi_j(\vec{r}) = \epsilon_j \phi_j(\vec{r}) , \tag{1}$$

$$n(\vec{r}) = \sum_j |\phi_j(\vec{r})|^2 F(\epsilon_j) , \tag{2}$$

where K is the kinetic energy operator and $F(\epsilon)$ is the Fermi function. Prescriptions for the construction of $v_{\text{eff}}(n,\vec{r})$ are extensively discussed in the literature.[6] For the evaluation of the Coulomb part of the potential we use the method developed by Weinert,[3] while for the exchange and correlation part we use the form of Hedin and Lundqvist.[7] In a pure material or an ordered alloy, the density $n(\vec{r})$ and, consequently, the potential $v_{\text{eff}}(n,\vec{r})$, have the periodicity of the underlying Bravais lattice. In that case, the construction of the density $n(\vec{r})$ according to Eq. (2) reduces to integrals over the first Brillouin zone, which we evaluate by employing the linear tetrahedron method.[8] The main emphasis of this section is on the solution of the differential equation (1).

The recognition that the charge density (or the potential) has a different characteristic behavior in different parts of the solid was an important step in the history of band-structure theory.[9] Near the atomic nucleus the core electrons are dominant and they give rise to an almost spherical charge density with pronounced features in the radial dependence. In the regions far from the nucleus the valence electrons are most important, leading to a charge density without much detailed structure. As a result, it is natural to define the so-called muffin-tin spheres, centered on the nuclei and with radii large enough to confine most of the core-electron charge density within the muffin-tin spheres, but restricted in that the muffin-tin spheres do not overlap each other. The obvious representations of the charge density (or the potential) in the resulting two distinct regions of space are

$$n(\vec{r}) = \sum_{\vec{G}} n(\vec{G})e^{i\vec{G}\cdot\vec{r}} \tag{3}$$

in the interstitial region, and

$$n(\vec{r}) = \sum_{l,m} n_{lm}(|\vec{r}-\vec{R}|)Y_{lm}((\vec{r}-\vec{R})/|\vec{r}-\vec{R}|) \tag{4}$$

within the muffin-tin sphere centered on the nucleus at position $\vec{R}$. The summation in Eq. (3) is over reciprocal lattice vectors $\vec{G}$. Traditional band-structure methods truncate one or both series after the first term, the latter resulting in the so-called muffin-tin approximation. This is a very reasonable approximation for close-packed metals (although for some transition metals like Nb the effects on the energy eigenvalues can be of the order of 10 mRy), but it breaks down severely for open structures and for materials with directed covalent bonds. Therefore, we have developed computer algorithms which are based on the full-potential linearized augmented plane wave method and which are similar in spirit to our existing film codes.[2,4] Our programs to solve the differential equation (1) do not contain any uncontrolled numerical approximations, and all series expansions and integrations are checked for sufficiently accurate convergence by increasing the number of functions or integration points (see the Appendix). As a result, the only approximations influencing our final results are connected to the use of local-density theory.

An important concept implemented in our approach to a full-potential (and fully relativistic) treatment is the introduction of a second variation. Given a (possibly spin-dependent) potential we first perform a semirelativistic, warped muffin-tin (WMT) self-consistent calculation which includes the full potential in the interstitial region but omits all nonspherical terms inside the muffin-tin spheres as well as spin-orbit coupling. The resulting wave functions are used as basis functions for a second variational calculation which includes all contributions to the potential which were left out in the first calculation. These contributions are only important inside the muffin-tin spheres and are of the form given by Eq. (4). Therefore, the main characteristic of the second variation is a linear transformation to an (l,m) representation of the wave functions:

$$\psi(n,\vec{k};\vec{R}+\vec{r}) = \sum_{l,m} \{a(n,\vec{k};l,m)R_l(E_l,r) + b(n,\vec{k};l,m)\dot{R}_l(E_l,r)\}Y_{lm}(\hat{r}) , \tag{5}$$

which is valid inside the muffin-tin sphere centered about $\vec{R}$. This is readily done in the spirit of the linearized augmented-plane-wave (LAPW) approach, where the functions R_l and $\dot{R}_l$ are the radial solutions to the semirelativistic Dirac equation and the energy derivative of this radial solution, respectively.[10] The coefficients a and b are obtained by a linear transformation from the coefficients C of the plane waves. In the interstitial region we have

$$\psi(n,\vec{k};\vec{r}) = \sum_{\vec{G}} C(n,\vec{k};\vec{G})e^{i(\vec{k}+\vec{G})\cdot\vec{r}} , \tag{6}$$

and the $a(n,\vec{k};l,m)$ and $b(n,\vec{k};l,m)$ are obtained by a reduction of the form

$$a(n,\vec{k};l,m) = \sum_{\vec{G}} C(n,\vec{k};\vec{G})A(\vec{G},\vec{k};l,m) , \tag{7}$$

where the matrices $\underline{A}$ can be expressed in terms of well-known analytic functions. The important aspect of this transformation is the resultant enormous increase in speed for the LAPW method. It is possible to include the $l \neq 0$ terms of Eq. (4) in the augmented-plane-wave (APW) basis, but this leads to a bilinear transformation between the $\vec{G}$ and the (l,m) representations, and becomes prohibitively slow for a large number of plane waves.

Since the additional terms are relatively small the Hamiltonian matrix for the second variation is already close to diagonal, implying that we do not have to incorporate many unoccupied states in our second variation. The exact number of these states is, of course, system dependent and has to be determined by standard convergence tests. It is good practice in the linearized APW method to choose the values of the energy parameters to lie at the center of the occupied bands, weighted according to angular decomposition inside the muffin-tin spheres. If the number of basis functions in the first variation is large enough the choice of these values for the energy parameters is not very critical and one easily obtains eigenvalues which are converged within 1 mRy for the whole range of the occupied bands. The unoccupied levels, on the other hand, are often located at larger distances from the energy-parameter values and are hence less well converged. However, this is of no concern, since the corresponding wave functions are only included in order to improve the quality of the occupied states in the second variational calculation and in this way they are folded back to energy levels in the vicinity of the parameter values where their description of the radial functions is optimal.

The concept of a second variation is even more powerful than presently used in our programs. First, the core and valence electrons are treated separately, resulting in a small nonorthogonality between their wave functions. Generally, this overlap is very small and can be neglected. However, in some surface calculations, a possible consequence of this enlarged variational freedom for the basis functions describing the valence band is an overestimation of the size of the work function, because the valence electrons are overbound. Second, the core electrons are treated fully relativistically using the spherical part of the potential only. Although this approach is very accurate for most levels, it sometimes leads to small deviations for some core electrons close to the valence band (like the $5p$ electrons in elements like[11] Cs) because these electrons have an appreciable density near the muffin-tin boundary and are therefore influenced by the nonspherical components of the potential. In addition, the overlap with neighboring electrons of the same type induces a dispersion of the energy levels involved. All effects mentioned in this paragraph can be incorporated in the second variation by including appropriate terms in the Hamiltonian and the overlap matrix.

Another way of treating the problematic energy core levels which lie close to the valence electrons is to evaluate them in the same way the valence electrons are treated. However, as is especially true for p electrons, such a semirelativistic treatment introduces an error due to the neglect of spin-orbit coupling. Fortunately, for a completely filled band the average effect of the spin-orbit in-

teraction is very small and often less important than the contributions to the total energy due to the energy dispersion in these higher-lying core levels. On the other hand, the nature of the calculation becomes more complicated when one treats such levels with their own set of energy parameters; this results in a division of the valence bands into two (or more) distinct energy windows.

III. TOTAL ENERGY STUDIES OF BCC AND FCC TUNGSTEN

In this section we focus primarily on the total energy (E_{tot}) and related quantities determined for bcc and fcc tungsten, because E_{tot} is an extremely sensitive measure of the accuracy of the calculation and hence will reflect the accuracy of our results most strongly. For reference, we also give electronic band structures, densities of states, and Fermi surfaces (Figs. 1—6). Our results reflect the typical structures found in bcc and fcc materials. A notable feature in the Fermi surface of bcc tungsten is the appearance of two small electron lenses along the symmetry line from Γ to H and from H to N. The shape of the first lens will change after the inclusion of the spin-orbit interaction because this lens is derived from bands which cross along the symmetry line from Γ to H in a semirelativistic treatment, but do not do so with spin-orbit coupling present. The resulting frequency in a de Haas—van Alphen measurement will be very small, on the order of 1 MG. The electron lens along the symmetry line from H to N is much less affected by the inclusion of the spin-orbit interaction and hence its response should be at a frequency of several MG.

Consider the more sensitive details of our calculations as embodied in E_{tot}. Figure 7 exhibits the electronic part of the E_{tot} as a function of the atomic volume. The upper two curves pertain to the fcc phase while the lower two curves refer to bcc tungsten. The dots represent our calculated values; the solid curves are parabolic fits to these data points. Note that there is a 25-mRy break in the en-
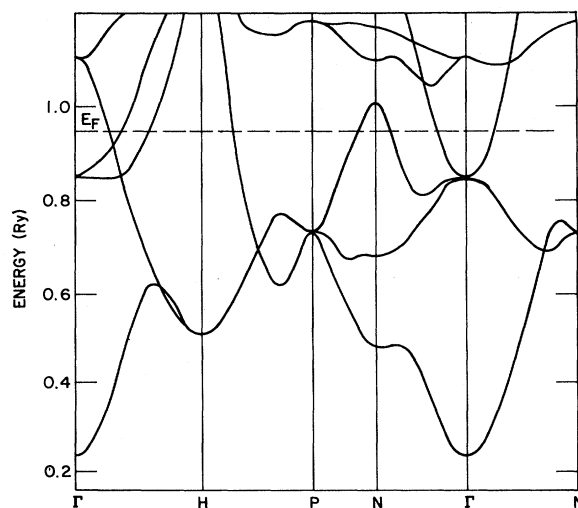

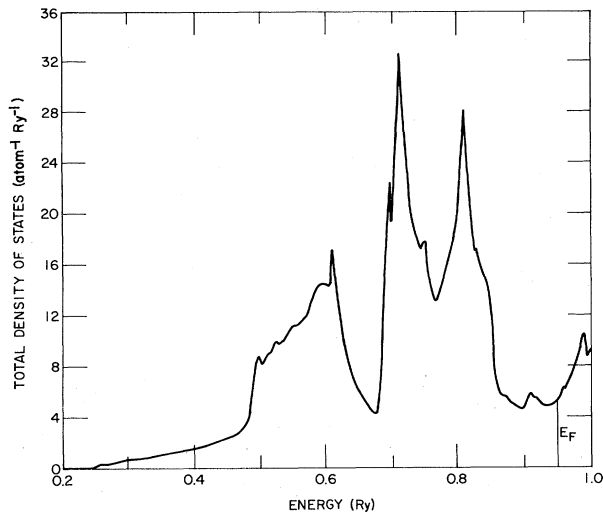FIG. 1. Electronic energy band structure of bcc tungsten for $a = 5.95$ a.u.

FIG. 2. Density of states of bcc tungsten for $a=5.95$ a.u. (in states/Ry atom).

FIG. 4. Electron energy band structure of fcc tungsten for $a=7.55$ a.u.

ergy scale. For each phase the top (bottom) curve is evaluated using 30 (90) $\vec{k}$ points in the irreducible wedge of the Brillouin zone (IBZ). The change in E_{tot} due to the change in the number of $\vec{k}$ points is different for fcc and bcc tungsten because of the different topology of the Fermi surface for these two structures. Tables I and II list the numerical results for our data points; Table III displays the minimal values of the total energy for the interpolating parabola. After extrapolating our results to an infinite number of $\vec{k}$ points (see the Appendix) we find an energy difference between fcc and bcc tungsten of 0.46 eV.

The equilibrium values of the lattice constants and the bulk moduli are listed in Table IV. These numbers are derived from the parabolic fits through the five data points; the results in the lines marked with an asterisk are obtained from a four-point fit, and omit the value at $a=6.10$ a.u. The values for the lattice constant are in good agreement with experiment; the error is less than 0.5%. Our results are smaller than the experimental values because we have neglected the slight overlap of the
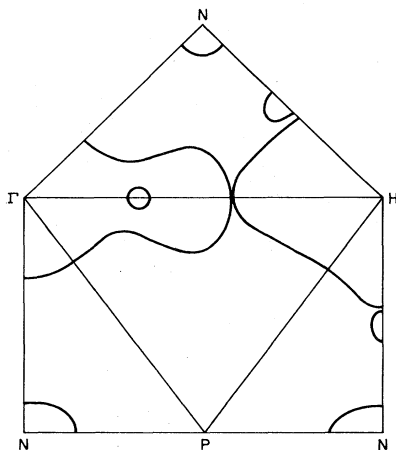
$5p$ core states in our calculation.

By contrast, the numbers for the bulk modulus scatter more widely around the experimental value, with a typical error ranging from 5% to 15%. However, the rms error of all our fits is less than 0.1 mRy, which corresponds to an uncertainty in the extracted values of the bulk modulus on the order of 1%. The large difference between the results of the four- and the five-point fit indicates that a parabolic form for the total-energy curve as a function of atomic volume is insufficient in the range of the lattice constants under consideration. Indeed, a careful analysis of the data shows a systematic deviation from the assumed quadratic dependence; at larger volumes the increase in the total energy is smaller than predicted by the quadratic formula and levels off towards the asymptotic atomic value. Therefore, we attribute the large discrepancies in the theoretical values of the bulk moduli compared to experiment to the use of an approximate form for the relation between the total energy and the atomic volume and not to an inaccuracy inherent in the FLAPW method or local-density theory.
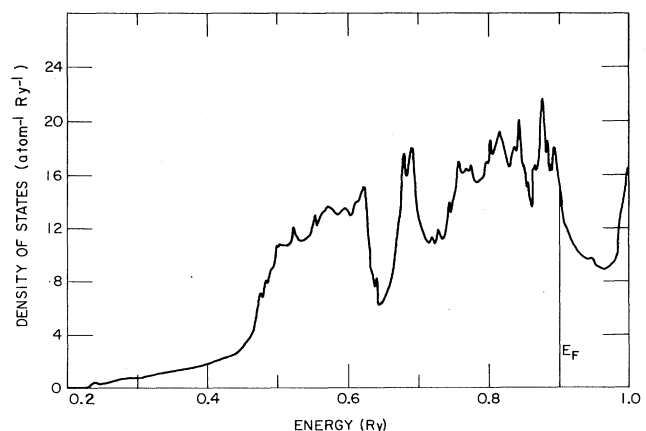

FIG. 3. Fermi surface of bcc tungsten for $a=5.05$ a.u.

FIG. 5. Density of states of fcc tungsten for $a=7.55$ a.u. (in states/Ry atom).
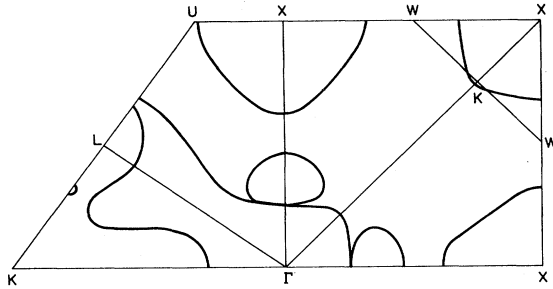
FIG. 6. Fermi surface of fcc tungsten for $a = 7.55$ a.u.

There appear to be two different ways to improve upon the present situation: First, one can restrict oneself to a smaller range of atomic volumes where a second order interpolation is valid. However, in this case, the corresponding energy range also becomes smaller and our relative error of 0.1 mRy in the total energy is no longer insignificant. Many data points are then needed in order to obtain an accurate value of the bulk modulus, because this quantity is a second-order derivative of the total energy and hence is very sensitive to numerical noise. A second, and much more promising way to handle the problem is to use a more realistic form of the total energy as a function of volume and to extend the range to larger atomic volumes. Our results show that this approach is feasible. The data point at $a = 6.10$ a.u. already deviates from a simple quadratic form near the equilibrium lattice con-
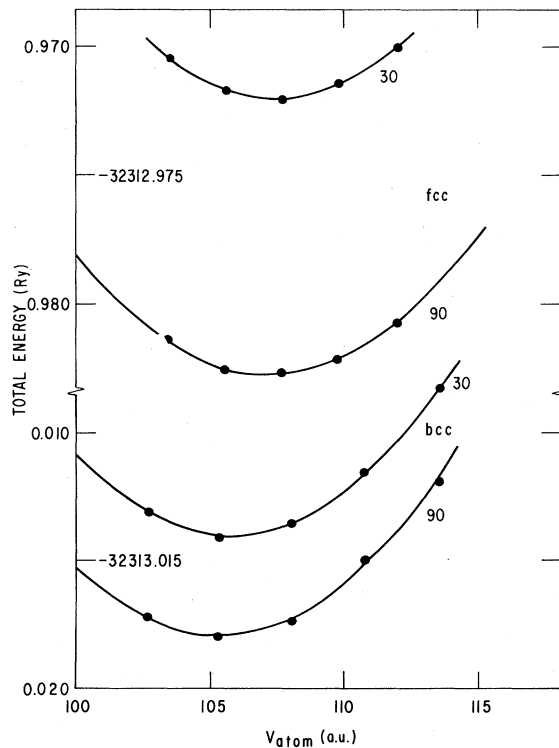

FIG. 7. Total energy versus atomic volume for bcc and fcc tungsten. The two curves in each case are for Brillouin-zone integrations using 30 on 90 points in the irreducible wedge. All values are in atomic units.

TABLE I. Total energy for bcc tungsten, in Rydberg atomic units.

a	V	$E_{tot}(30)$	$E_{tot}(90)$
5.90	102.6895	$-32\,313.0131$	$-32\,313.0172$
5.95	105.3224	$-32\,313.0141$	$-32\,313.0180$
6.00	108.0000	$-32\,313.0135$	$-32\,313.0173$
6.05	110.7226	$-32\,313.0115$	$-32\,313.0149$
6.10	113.4905	$-32\,313.0083$	$-32\,313.0118$

stant. This indicates that even at a lattice expansion of only 3%, higher-order terms in the polynomial relation between total energy and atomic volume are important. In order to determine the parameters describing these higher-order terms one does not need to perform calculations for values of the lattice constant which are substantially different from the equilibrium value (e.g., expansions on the order of 50%), in which case the computational effort would increase enormously. Now a 1% change in the lattice constant does not affect the charge density in a dramatic way and so only a few iterations are needed to arrive at the self-consistent density for the new value of the lattice constant. However, a 10% increase is large in the sense that starting from the previous charge density (or from a charge density constructed from overlapping atomic densities) essentially requires the same large number of iterations to obtain a self-consistent solution as was required originally.

In these sets of calculations we neglected the dispersion of the $5p$ electrons by treating them as core electrons. Therefore, we also performed a series of calculations in which these electrons were treated on the same footing as the valence electrons, that is including nonspherical terms and overlap but neglecting spin-orbit coupling. The resulting values of the lattice constant and the bulk modulus were the same within the errors of 0.5% and 15%, respectively, indicating that the cohesive effects of these electrons are small at the equilibrium lattice constant. Of course, for smaller values of the lattice constant the $5p$ electrons will start to add an important repulsive term to the total energy. The width of the $5p$ band is about 80 mRy and the nonspherical terms change the energy eigenvalues by less than 0.1 mRy. The wave functions of these states are very localized and a large number of plane waves are needed for an accurate description. This requirement of a large number of plane waves is also reflected in the extreme sensitivity of the total energy with respect to the choice of the value of the energy parameter describing the $5p$ band. Even in our case where we use many basis functions (on the other of 140), a change of 5 mRy in the $5p$ energy parameter (which is small com-

TABLE II. Total energy for fcc tungsten, in Rydberg atomic units.

a	V	$E_{tot}(30)$	$E_{tot}(90)$
7.45	103.3734	$-32\,312.9704$	$-32\,312.9814$
7.50	105.4687	$-32\,312.9717$	$-32\,312.9826$
7.55	107.5922	$-32\,312.9720$	$-32\,312.9826$
7.60	109.7440	$-32\,312.9714$	$-32\,312.9821$
7.65	111.9243	$-32\,312.9700$	$-32\,312.9807$

TABLE III. Equilibrium values of the total energy in Rydberg atomic units.

bcc (30)	−32 313.0140
bcc (90)	−32 313.0179
bcc (∞)	−32 313.0186
fcc (30)	−32 312.9720
fcc (90)	−32 312.9827
fcc (∞)	−32 312.9847

pared to the bandwidth) can cause a change in E_{tot} of the same order of magnitude because in the process, the whole $5p$ band shifts up or down. On the other hand, a change of 0.2 Ry in the energy parameters describing the valence band changes E_{tot} by less than 0.1 mRy, indicating that the range of accuracy of the linearized method is large enough to describe the whole occupied part of the valence band. For systems with spatially localized electrons in completely filled bands which are treated like valence bands it thus appears to be a general feature that the total energy is very sensitive to the precise position of these bands. Hence, greater care must be taken in arriving at a consistent description in such a situation.

IV. CONCLUSIONS

We have shown that very accurate total-energy calculations using the full-potential linearized augmented-plane-wave method are feasible and lead to predictions which can be compared directly with experiment. As further spelled out in the Appendix, our method controls the effect of all numerical approximations and truncations. Consequently, our results reflect the accuracy of the theoretical approximations to the exchange and correlation energy which are used in the calculation. Compared to calculations which only aim at providing a description of electronic band properties like the Fermi surface, the evaluation of reliable values of the total energy requires a larger computational effort because of the increase in nu-

TABLE IV. Comparison of equilibrium lattice constants and bulk moduli (in atomic units). The lines marked with an asterisk are results obtained from a four-point fit and omitting the value at $a = 6.10$ a.u.

	a_0	B
bcc (30)	5.957	2.00×10^{-2}
bcc (90)	5.949	1.92×10^{-2}
bcc (∞)	5.947	1.90×10^{-2}
bcc (30)*	5.958	2.20×10^{-2}
bcc (90)*	5.952	2.33×10^{-2}
bcc (∞)*	5.951	2.35×10^{-2}
(Ref. 12)	5.975	2.02×10^{-2}
(Ref. 13)	5.996	2.35×10^{-2}
Experimental	5.973	2.20×10^{-2}
fcc (30)	7.545	2.13×10^{-2}
fcc (90)	7.539	1.90×10^{-2}
fcc (∞)	7.538	1.86×10^{-2}

merical accuracy. For example, the size of the secular matrix has to be enlarged by at least a factor of 2.

The total-energy FLAPW approach enables the prediction of structural properties. Lattice parameters are quite accurately predicted. Calculated total energies have a relative precision of 0.1 mRy, which is equivalent to a temperature of 16 K. In many cases, this is a small number compared to the energy difference between several crystal phases. For tungsten, we found a difference of 34 mRy between the (stable) bcc and fcc phases.

Finally, we have found that this approach allows one to calculate the value of the electronic part of the total energy as a function of the volume with sufficient accuracy to investigate the validity of different models used to describe this dependence. In the case of tungsten, we have shown that the use of a simple quadratic form near the equilibrium value of the atomic volume can lead to relatively large errors for the bulk modulus. An improved model description of this relation for larger values of the atomic volumes should also lead to accurate predictions concerning the cohesive energy, which by definition is equal to the difference in total energy between the equilibrium configuration and the system at infinite volume. A reliable value of the cohesive energy is certainly possible within the framework of our total-energy FLAPW approach provided an equally accurate[4] local-spin-density calculation is obtainable for the isolated atom.

Note added in proof. Since submitting this paper, we completed an accurate computer program for the evaluation of the electronic structure of spin-polarized atoms in which the orbitals are treated either fully- or semi-relativistically. The calculated values for the total energy of a tungsten atom in the local-density approximation were (i) −32 312.218 Ry for a fully-relativistic atom, (ii) −32 312.086 Ry for a calculation in which the valence $5d$ and $6s$ orbitals were treated semi-relativistically and were nonpolarized, and (iii) −32 312.300 Ry when allowing the semi-relativistic $5d$ and $6s$ electrons to fully polarize into a $d^5 s^1$ configuration. Use of the last number resulted in a value of the cohesive energy of 9.76 eV/atom, which is about 10% larger than the experimental value, 8.90 eV/atom. As in other accurate local-density approximation underestimates the contribution to the total energy of the valence electrons in the atom, which become more strongly localized and have low-density tails far from the nucleus.

ACKNOWLEDGMENTS

APPENDIX

One very important aspect of the FLAPW method for solving the Kohn-Sham equations is the absence of uncon-

trolled numerical parameters. In essence, this means that we are always able to calculate the accuracy of our results and that we know how to make improvements when the errors are too large. In a numerical implementation of any algorithm one always has to replace infinite series and continuous integrations by finite sums, which leads to numerical errors. By increasing the number of terms the deviations become smaller, very often according to known analytical laws. This is especially important in cases where limits on computational time actually inhibit calculations of sufficient accuracy; one then uses the analytic convergence laws to predict well-converged results. Of course, the foregoing discussion only applies to numerical errors and does not pertain to the effect of physical approximations, like the use of local-density functionals. Therefore, the FLAPW method is very well suited for testing the quality of various implementations of density-functional theory, exactly because it minimizes all numerical errors.

In this appendix we make a distinction between the effects of the nonspherical terms inside the muffin tins and all other numerical truncations, because the full-potential capability is a new aspect of our approach. The effects of the introduction of nonspherical terms on the eigenvalues is shown in Table V for a typical case of bcc Nb. Our results are consistent with this earlier work of Elyashar and Koelling.[14] Of course the change in eigenvalues becomes larger for systems with lower symmetry; on the other hand, for fcc W which is a system of very high symmetry the changes in the eigenvalues are only of the order of 1 mRy. In this last case the first nonspherical term in the density and in the potential has $l=4$.

The total energy of the electronic system is a much more sensitive parameter and in most cases it is the important quantity to monitor. Even in fcc W the total energy pertaining to the self-consistent density changes by 5 mRy after introducing the $l=4$ terms. Although this difference does not seem very large, it is comparable to the size of energy differences of physical interest and hence the inclusion of these terms is important. The combined effects of the $l=6$ and 8 terms on the total energy is less than 0.5 mRy. Since the high-l terms typically scale like $(r/R_{MT})^l$ we see that the effect of higher-order terms rapidly becomes smaller. Hence, including nonspherical terms up to $l=8$ is sufficient for most simple systems with cubic symmetry. Finally, our experiences with several cubic systems with one atom per unit cell shows

that the matrix of the second variation is already nearly diagonal. In these cases we only have to incorporate a small number of unoccupied states to obtain a well-converged result for the total energy. Typically, we include states up to 1–2 Ry above the Fermi level, leading to matrix sizes between 10 and 20 for transition metals. Of course for more complicated systems one has to reassess this question.

We now focus on the numerical parameters which enter into any LAPW calculation. A quantity inherent to the linear methods is the energy parameter; this gives the value at which the radial integrations are performed. The accuracy of the description of the valence band decreases when the corresponding energy eigenvalues deviate more and more from the value of the energy parameters. Since the energy parameters are l dependent, different subbands can have different ranges of high accuracy. The error resulting from the linearization is easily found: changing the values of the energy parameters will immediately show the sensitivity of the results with respect to this choice. Formally, the way to improve the quality of the energy bands is to incorporate second-order energy derivatives into the description of the wave functions inside the muffin tins. But this changes the nature of the programs completely. However, since the LAPW method is variational in nature, one can also minimize the error by increasing the number of basis functions. It is our experience that for transition metals with one atom per unit cell a basis set with approximately 100 augmented plane waves is sufficiently large to yield a total energy which changes by less than 0.1 mRy when varying the value of the energy parameter over the entire range of the occupied d band.

Two parameters which are easy to control by making their values large enough are the number of plane waves (needed for the description of the charge density and the potential in the interstitial region) and the maximum l value (used for the augmentation of the plane waves inside the muffin tin). The first parameter is chosen in such a way that all combinations of reciprocal lattice vectors used in the set of basis functions are incorporated into the expansions in the interstitial region. For the second, a value of $l_{max}=8$ turned out to be sufficient for an accurate representation of the radial functions of transition metals. Changing this value to 12 in tungsten caused a systematic shift of the total energy by 0.2 mRy. However, in an insulating material like SrS the corresponding change was 3.4 mRy because the whole valence band was shifted down in energy due to the increased accuracy of the basis functions.

Another pair of numerical parameters which can be chosen large enough to ensure sufficient accuracy pertain to the radial mesh employed in the radial integrations; however, some care is required. In our programs we generally use a radial mesh with a logarithmic step of 0.03 and 361 mesh points. The resulting error in the total energy due to inaccuracies in the valence band is of order 0.1 mRy, as was easily tested by performing calculations for metallic hydrogen and lithium. However, a problem arises because of the extreme localization of the 1s core levels in heavy materials like tungsten. Their wave func-

TABLE V. Change in energy eigenvalues in mRy for bcc Nb due to nonspherical terms; RAPW represents the relativistic augmented plane wave.

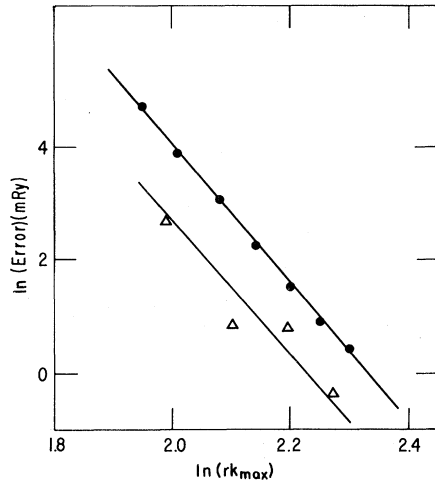| This work		RAPW (Ref. 14)	
Γ_1	$+0.5$	Γ_6^+	$+0.1$
Γ_{25}'	-9.0	Γ_8^+	-5.3
		Γ_7^+	-5.4
Γ_{12}	$+8.5$	Γ_8^+	$+5.2$
H_{12}	$+8.0$	H_8^+	$+5.1$
H_{25}'	-1.7	H_8^+	-1.2
		H_7^+	-1.3

FIG. 8. Numerical error in the total energy resulting from the use of a finite basis for bcc tungsten $(\triangle)$ and a mercury monolayer $(\bullet)$.

FIG. 9. Numerical error in the total energy resulting from the use of a finite number of points in the Brillouin-zone integrations for bcc tungsten $(\triangle)$, a mercury monolayer $(\bullet)$, and simple cubic hydrogen $(\bigcirc)$.

tions extend only over a small number of mesh points, inducing errors in the total energy in the mRy range. On the other hand, the $1s$ core levels are chemically completely inactive and do not change under a structural transformation. Therefore, as long as one retains the same radial mesh in all the calculations, the error in the total energy as dictated by the changes in the valence electrons becomes systematic and energy differences are then accurate to within 0.1 mRy.

Finally, we turn to the numerical parameters on which the most extensive tests have to be performed repeatedly for every new system. These are the number of basis functions and the number of k points in the irreducible wedge of the Brillouin zone. The number of basis functions is conventionally determined by the quantity rk_{max}, which is the product of an average value of the muffin-tin radius and a sphere radius k_m in reciprocal space. For a given point $\vec{k}$ our basis set includes all reciprocal lattice vectors $\vec{G}$ with $|\vec{k}-\vec{G}| < k_m$. In Fig. 8 we plot the logarithm of the error in the total energy versus the logarithm of rk_{max} for a monolayer of mercury and for bcc tungsten. In the case of W reciprocal lattice vectors were determined by $G < k_m$, which leads to a more discontinuous behavior since some shells of reciprocal lattice vectors contribute less than others. Emerging from this plot is a power-law behavior for the error as a function of rk_{max}, with a rather large value of the exponent, roughly -14. We have checked that a fit to an exponential form leads to a larger RMS error of the data points. We do not know the analytical basis for this power law for the error; it will be interesting to see if a theoretical deviation will indeed lead to large exponents. Also it follows that the number of plane waves necessary to obtain an absolute error in the total energy of less than 1 mRy is of order 100 (for a one atom per unit-cell calculation), although the relative errors are much smaller. The precise number will depend on the ratio of the interstitial volume and the total unit-cell volume, but it is already clear that in order to obtain a well-converged value of the total energy one requires
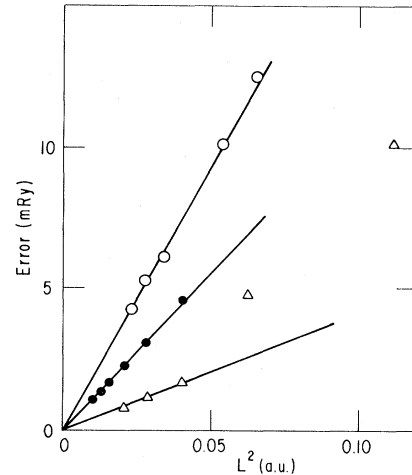
many more basis functions than is required to obtain a well-converged Fermi surface, which requires about 30—40 augmented plane waves per atom. Of course, a large number of basis functions is only needed in the final iterations when one is close to self-consistency.

The last quantity we consider is the number of $\vec{k}$ points in the irreducible wedge of the Brillouin zone. This parameter enters because we employ the linearized tetrahedron method for the integrals in reciprocal space which enter into the construction of the charge density and the total energy. The number of $\vec{k}$ points becomes a numerically important parameter especially when we want to (i) compare the total energies of different structures with different Fermi-surface topologies or (ii) trace the value of the total energy through a metal-insulator transition. In the linearized tetrahedron method, the error in the total energy scales with L^2, where L is a typical dimension of a tetrahedron. This behavior is beautifully confirmed in Fig. 9 where we plot results for metallic hydrogen, tungsten, and a mercury monolayer[15] (in the last case we use triangles instead of tetrahedrons since its reciprocal space is two dimensional). In tungsten, the data points for a low number of $\vec{k}$ points deviate from the straight line due to a Fermi-surface effect; there is a small electron lens on the symmetry line from Γ to H, and only when we have enough $\vec{k}$ points to properly describe this lens does the total energy follow its asymptotic behavior. The actual number of $\vec{k}$ points needed to obtain an error in the total energy of less than 1 mRy is about 200 for bcc tungsten and about 3000 for metallic hydrogen. (In the latter case the number is very large because there are no compensating effects between electron and hole sheets in the almost spherical electron Fermi surface.) One clearly sees that the knowledge of the error law greatly facilitates the calculations, although a careful analysis of the Fermi surface is required.

Because of the numerical integrations over the Brillouin zone appearing in the construction of the charge density,

the output density is not neutral up to machine precision. Depending on the system studied, the total charge inside a Wigner-Seitz cell will be somewhere between 10^{-6} and 10^{-10}. Deviations from charge neutrality larger than 10^{-6} result in a noticeable error in the total energy of more than 1 mRy. It therefore becomes necessary to make the output density neutral up to machine precision by adding or subtracting the excess charge. Since the er- ror in the charge normalization is strictly due to the valence electrons, the excess charge will be distributed almost uniformly over the unit cell. Hence, restoring charge neutrality can be done homogeneously because the remaining effects which are related to the neglect of all structure of the excess charge have a much smaller magnitude.

---

[1]P. Hohenberg and W. Kohn, Phys. Rev. **136**, B864 (1964); W. Kohn and L. J. Sham, *ibid.* **140**, A1133 (1965).

[2]E. Wimmer, H. Krakauer, M. Weinert, and A. J. Freeman, Phys. Rev. B **24**, 864 (1981).

[3]W. Weinert, J. Math. Phys. **22**, 2433 (1981).

[4]M. Weinert, E. Wimmer, and A. J. Freeman, Phys. Rev. B **26**, 4571 (1982), and references therein.

[5]See also M. C. Huang, H. J. F. Jansen, and A. J. Freeman, Bull. Am. Phys. Soc. **28**, 343 (1983).

[6]See, for example, W. Kohn and P. Vashista, in *Theory of the Inhomogeneous Electron Gas,* edited by S. Lundqvist and N. M. March (Plenum, New York, 1983), p. 79; A. K. Rajagopal, Adv. Chem. Phys. **41**, 59 (1980).

[7]L. Hedin and B. I. Lundqvist, J. Phys. C **4**, 2064 (1971).

[8]J. Rath and A. J. Freeman, Phys. Rev. B **11**, 2109 (1975); G. Lehman and M. Taut, Phys. Status Solidi **54**, 469 (1972); O. Jepson and O. K. Andersen, Solid State Commun. **9**, 1763 (1971).

[9]J. C. Slater, Phys. Rev. **51**, 846 (1937).

[10]D. D. Koelling and G. O. Arbman, J. Phys. F **5**, 2041 (1975); O. K. Andersen, Phys. Rev. B **12**, 3060 (1975); A. H. MacDonald, W. E. Pickett, and D. D. Koelling, J. Phys. C **13**, 2675 (1980); O. K. Andersen, in *The Electronic Structure of Complex Systems,* edited by W. Temmerman and P. Phariseau (Plenum, New York, 1982).

[11]E. Wimmer, Surf. Sci. **134**, 487 (1983).

[12]D. M. Bylander and L. Kleinman, Phys. Rev. B **27**, 3152 (1983).

[13]A. Zunger and M. L. Cohen, Phys. Rev. B **19**, 568 (1979).

[14]N. Elyashar and D. D. Koelling, Phys. Rev. B **13**, 5362 (1976).

[15]H. J. F. Jansen, A. J. Freeman, M. Weinert, and E. Wimmer, Phys. Rev. B **28**, 593 (1983).